

Supporting information

A single-molecule atomic force microscopy study reveals the antiviral mechanism of tannin and its derivatives

Huijie Wang, Ying Chen, Wenke Zhang*

State Key Laboratory of Supramolecular Structure and Materials, Jilin University, Changchun,
130012, P. R.China.

* Corresponding author: zhangwk@jlu.edu.cn

The estimation of the effective contact area by using Hertz model¹.

$$a = \left(\frac{3PR}{4E^*} \right)^{\frac{1}{3}}, R = \frac{R_1 R_2}{R_1 + R_2}, E^* = \frac{1}{\frac{1}{E_1} + \frac{1 - \nu_1^2}{E_1} + \frac{1 - \nu_2^2}{E_2}}$$

Where a , R_1 , R_2 , E_1 , E_2 , ν_1 , ν_2 are the contact radius, the tip radius, outer radius of TMV, Young's modulus of tip and TMV, the Poisson's ratio of tip and TMV.

We know $R_1=20$ nm, $R_2=9$ nm. From the work by Zhao et al.² we know $E_1=155$ GPa, $E_2=1$ GPa, $\nu_1=0.27$, $\nu_2=0.48$. In our experiment the external force $P=1$ nN, so contact radius $a=1.5$ nm, contact area $A=\pi a^2=7.1$ nm²

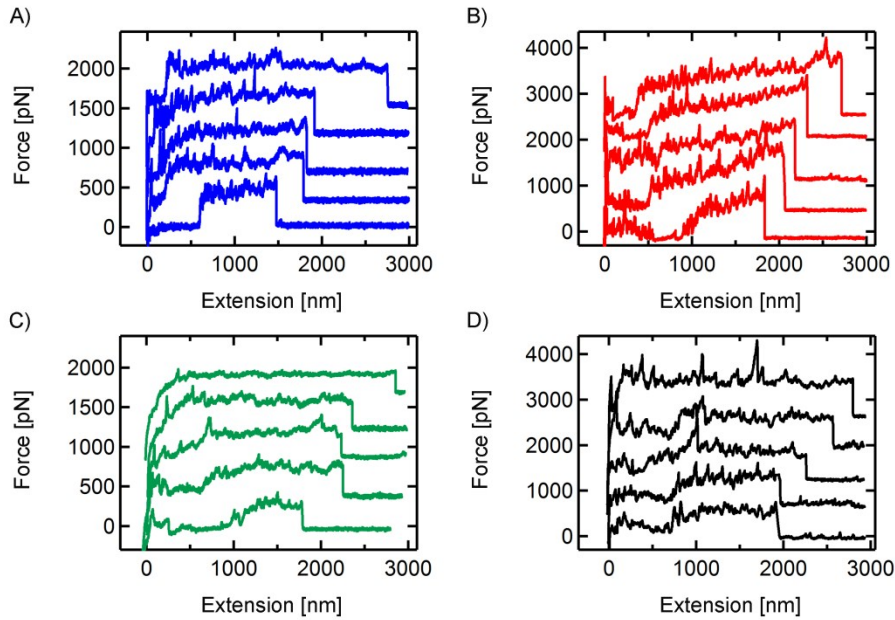


Fig. S1. Representative force-extension curves obtained during the pulling of RNA out of TMV particle in the absence of tannin at (A) pH 4.7 (blue curves), (C) pH 7.0 (green curves), and in the presence of tannin at (B) pH 4.7 (red curves), (D) pH 7.0 (black curves) at a pulling speed of 2.0 μ m/s.

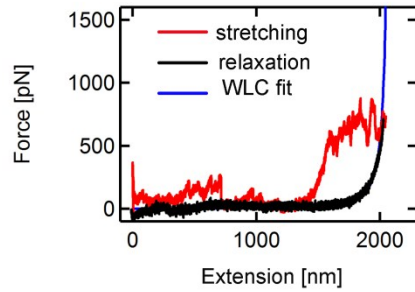


Fig. S2. Typical stretching and relaxation curves of TMV in the presence of tannin at pH 4.7 superimposed with a WLC fit (blue solid curve) below 200 pN. A worm-like chain (WLC)³ fit to the relaxation curve produced a persistence length of ~ 0.68 nm, which is very close to that of a single RNA chain.⁴⁻⁸ So we can conclude that the plateau in the stretching curve corresponds to the disassembly of the a RNA from its protein coat by the external force.

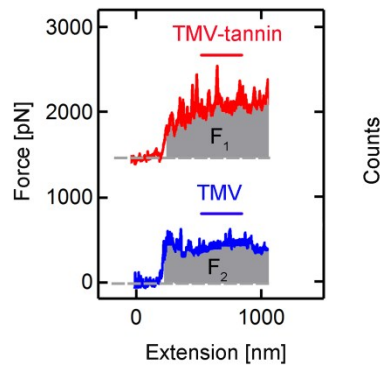


Fig. S3. Standard for the measurement of rupture forces. The two force-extension curves represent the data obtained in the absence (blue curve) and presence of tannin (red curve) at pH 4.7 at a pulling speed of $2 \mu\text{m/s}$. We statistically analyzed the force on all the data points in the sawtooth plateau region as marked by the shade to determine the unbinding force.

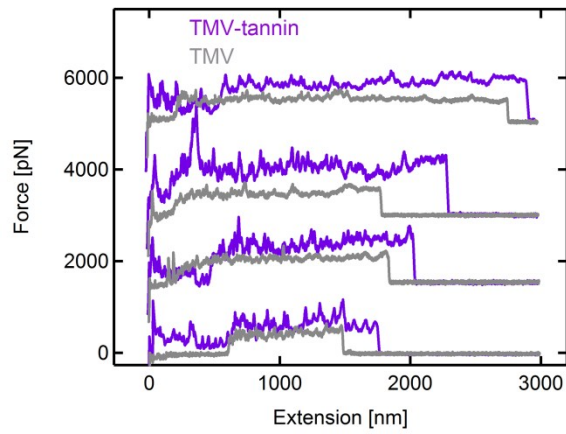


Fig. S4. A comparison of typical sawtooth-plateau-containing force-extension curves obtained during the disassembly of RNA from TMV particles in the absence (grey curve) and presence of tannin (purple curve) at pH 4.7.

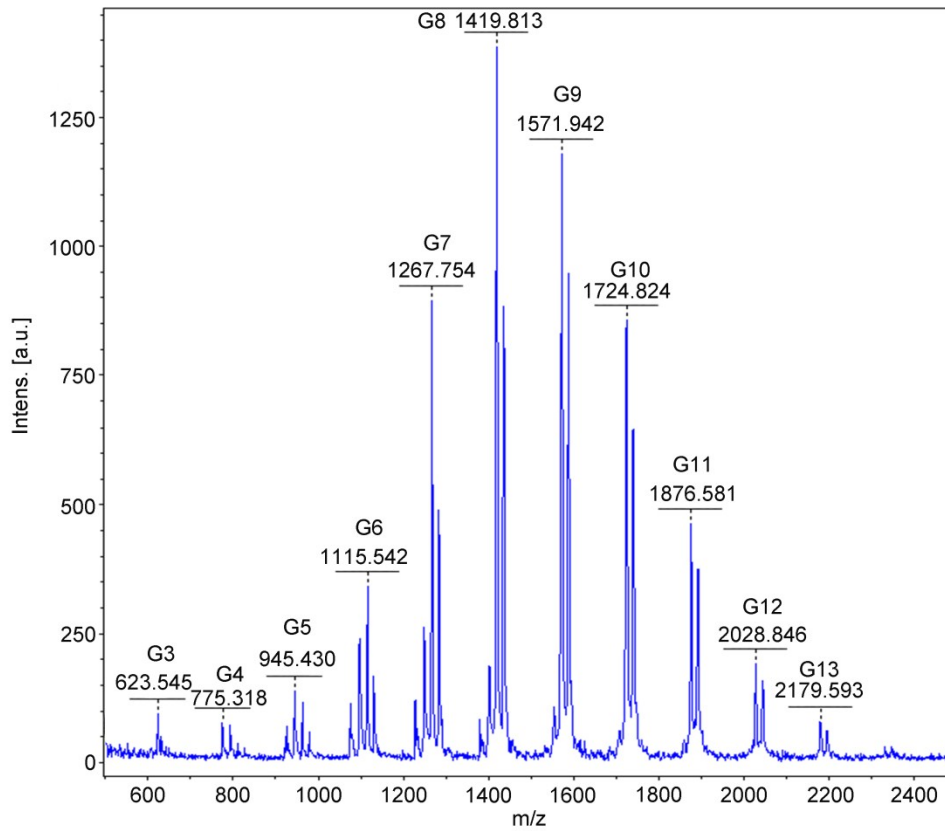


Fig. S5. MALDI-TOF mass spectra of gallotannin. Gn corresponds to polygalloylglucoses containing n (n=3...13) galloyl groups.

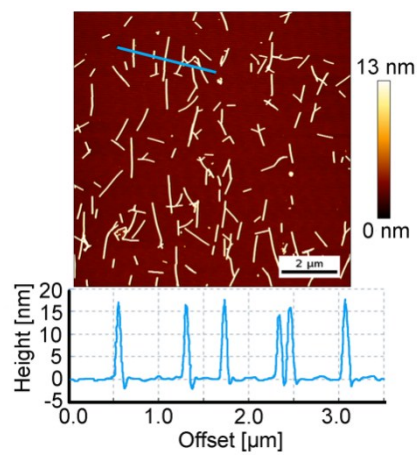


Fig. S6. AFM topography images of TMV (0.01 mg/ml). The blue line in the AFM image represents the site of the section analysis that is depicted in the panel below.

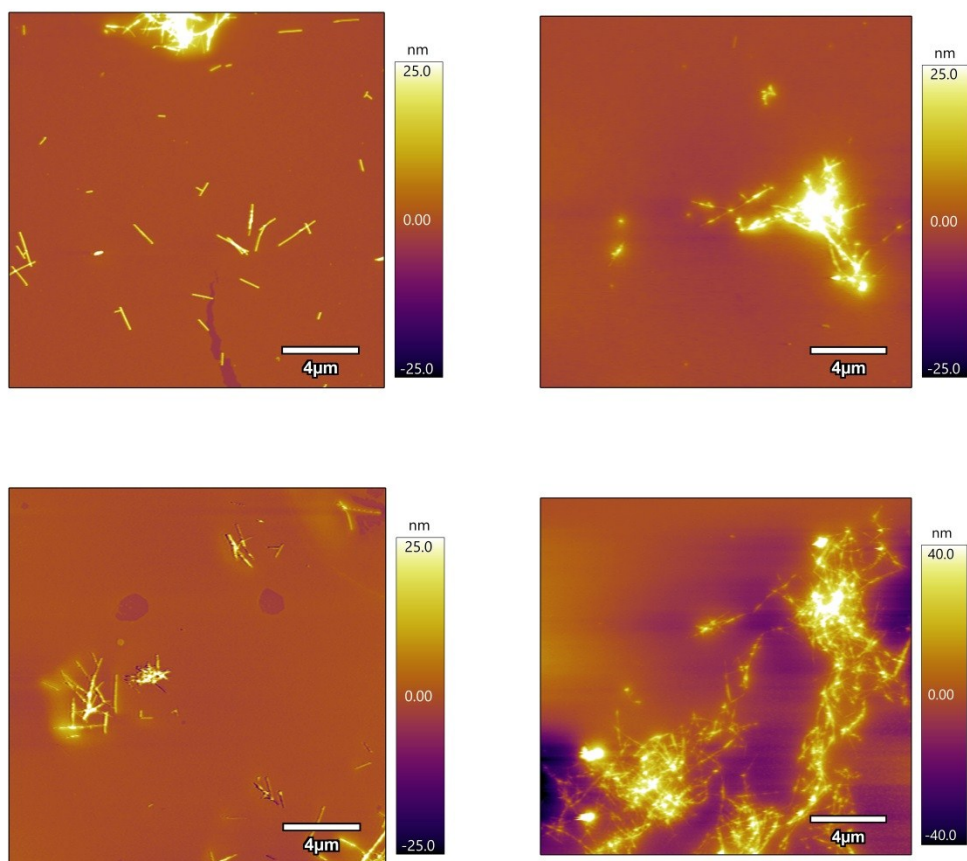


Fig. S7. More AFM topography images of TMV obtained in the presence of 22.5 mg/ml tannin.

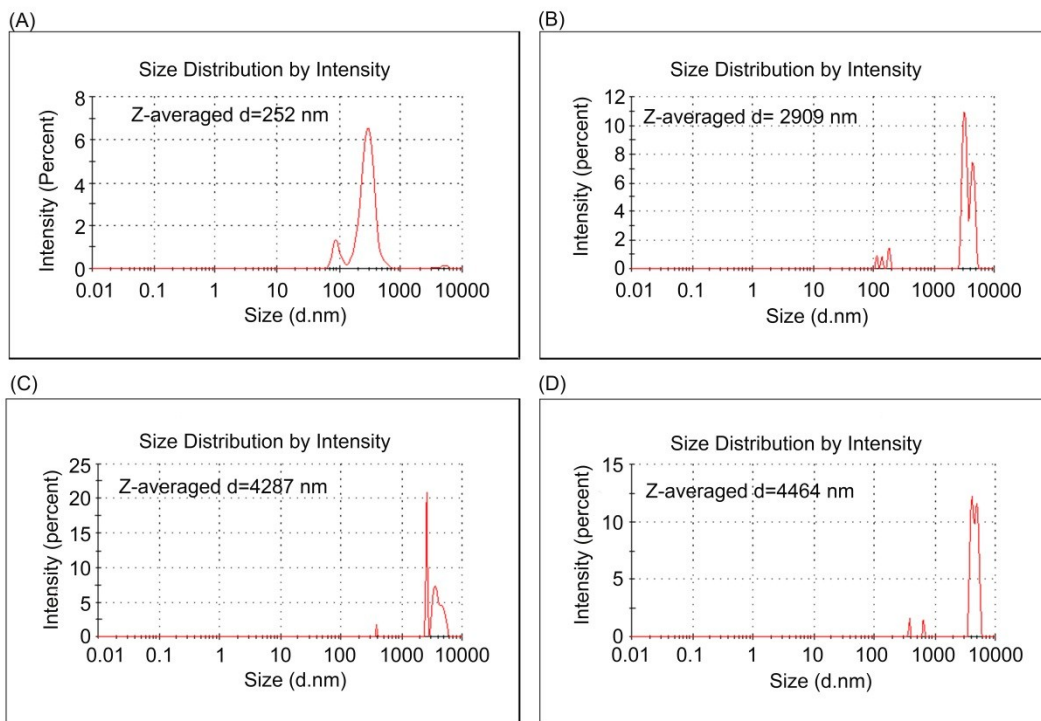


Fig. S8. The size distribution of TMV particles (A) in the absence and in the presence of (B) 0.098 mg/ml, (C) 0.98 mg/ml and (D) 4.9 mg/ml of tannin.

We measured the particle size in the presence of different concentration of tannin by photon correlation spectroscopy (PCS) with a NanoZS90 Zetasizer (Malvern Instruments Ltd.) During the measurement 1 μ l of TMV solution (25 mg/ml) was mixed with 49 μ l of PBS containing tannin 0 mg/ml, 0.1 mg/ml, 1.0 mg/ml, 5 mg/ml, respectively to get a final TMV concentration 0.5 mg/ml, final tannin concentration 0 mg/ml, 0.098 mg/ml, 0.98 mg/ml, 4.9 mg/ml. The PCS results show that with the increase of tannin concentration, the Z-averaged hydrodynamic diameters become larger indicative of the tannin-induced TMV aggregation.

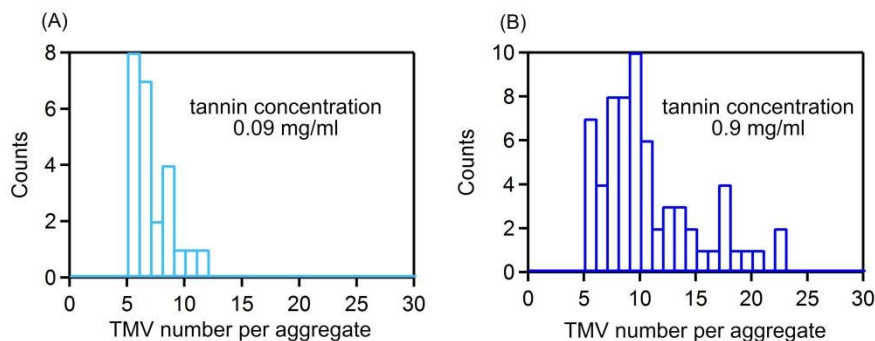


Fig. S9. The number distributions of TMV particles per aggregate in the presence of (A) 0.09 mg/ml and (B) 0.9 mg/ml of tannin.

We defined particle containing more than 4 TMV as aggregate. Then we calculated the total number of aggregates in 36 AFM images ($10 \times 10 \mu\text{m}$) and the total number of TMV particles in these aggregates. So we can get the average number of TMV particles in an aggregate. We also counted the number of TMV particles in every aggregate. Then we got the number distribution of TMV particle in each aggregate. According to AFM images, there is no aggregate in pure TMV. The aggregation of TMV is severe in the presence of 22.5 mg/ml tannin (Figure 5E and Figure S7), as a result it is difficult to count the number of TMV particles under this condition. For the case in Figure 5C, in the presence of 0.09 mg/ml of tannin, the number distribution of TMV particles in each aggregate is in the range of 5-11 (Fig. S9A), with an average number of 6. For the case in Figure 5D, in the presence of 0.9 mg/ml of tannin, the number distribution of TMV particles in each aggregate is in the range of 5-22 (Fig. S9B), with an average number of 10.

Reference

- (1) K. L. Johnson, K. Kendall, A. D. Roberts, *Proc. R. Soc. Lond. A.*, 1971, **324**, 301-303.
- (2) Y. Zhao, Z. Ge, J. Fang, *Phys. Rev. E*, 2008, **78**, 031914(1-5).
- (3) W. Zhang, X. Zhang, *Prog. Polym. Sci.*, 2003, **28**, 1271-1295.
- (4) N. Liu, B. Peng, Y. Lin, Z. Su, Q. Wang, W. Zhang, H. Li, J. Shen, *J. Am. Chem. Soc.*, 2010, **132**, 11036-11038.
- (5) S. B. Smith, Y. Cui, C. Bustamante, *Science*, 1996, **271**, 795-798.
- (6) M. Rief, H. Clausen-Schaumann, H. E. Gaub, *Nat. Struct. Biol.*, 1999, **6**, 346-349.
- (7) S. X. Cui, J. Yu, F. Kühner, K. Schulten, H. E. Gaub, *J. Am. Chem. Soc.*, 2007, **129**, 14710-14716.
- (8) H. Chen, S. P. Meisburger, S. A. Pabit, J. L. Sutton, W. W. Webb, L. Pollack, *PNAS*, 2012, **109**, 799-804.